8-Aza-3-deazaguanine modification strengthens the anomeric effect and affects other conformational preferences of modified guanine nucleosides

Miha Plevnik, Martin Črnugelj, Anton Štimac, Jože Kobe and Janez Plavec*

National Institute of Chemistry, Hajdrihova 19, SI-1115, Ljubljana, Slovenia.
E-mail: janez.plavec@ki.si

Received (in Cambridge, UK) 23rd November 2000, Accepted 4th June 2001
First published as an Advance Article on the web 5th July 2001

A variable temperature-dependent ^{1}H NMR conformational analysis of $^3J_{HH}$ coupling constants and NOE enhancements of a series of 8-aza-3-deaza modified guanine nucleosides **2** and **4**–**8** has been performed in DMSO-d_6 and the results compared to those for natural nucleosides dG (**1**) and G (**3**). 8-Aza-3-deaza nucleobase modification leads to the stabilization of N-type conformers by $\Delta\Delta H°$ of 3.1 kJ mol^{-1}, which has been attributed to the strengthening of the O4′–C1′–N9 anomeric effect. The strengthening of the anomeric effect of 8-aza-3-deazaguanine compared to guanine is explained by the redistribution of electron density from N9 into the pyridine moiety which facilitates $n_{O4'} \rightarrow \sigma^*_{C1'-N9}$ orbital interactions. The anomeric effect of 8-aza-3-deazaguanine in 8a3d-dG (**2**) is approximately 19.5 kJ mol^{-1} with the assumption that the steric effects of nucleobases in dG (**1**) and 8a3d-dG (**2**) are comparable. 2′- and 3′-Substituents drive the N $\rightleftharpoons$ S equilibrium *via* their involvement in *gauche* effects, which are only moderately affected by the nucleobase modification. The 2′-OH group in ribo (**4**), xylo (**7**) and 3′-deoxyribo (**8**) counterparts, however, drives the N $\rightleftharpoons$ S equilibrium towards S by the *gauche* effect of the [N9–C1′–C2′–O2′] fragment, which has been strengthened by $\Delta\Delta H°$ of 1.8 kJ mol^{-1} due to 8-aza-3-deaza nucleobase modification. 2′-F in the arabino analogue 8a3d-FaraG (**6**) showed conformational preferences which are nucleobase specific and could not be attributed to the *gauche* effects. The larger population of γ^t rotamers in **1**–**8** correlates with the larger population of N-type conformers.

Introduction

Structural modifications of natural nucleobases can influence basic biochemical processes like metabolism of nucleic acid constituents as well as their normal functions. Nucleobase modifications have been extensively used in the search for antiviral and antitumor active compounds. 3-Deazaguanine is a potent guanine antimetabolite with significant antitumor and antiviral activities.[1] Various ring and sugar modifications on 3-deazaguanosines have been made,[2–4] resulting in a wide modulation of the biological activity. Nucleobase modified nucleosides are, in addition, potentially important as probes in studies of mechanisms and catalytic activities of individual functional groups[5,6] or as an aid in NMR assignments. An antisense oligonucleotide has to adopt an A-type conformation with characteristic N-type sugar puckering for higher affinity to the RNA target, which can be achieved by the nucleobase modifications that also influence pairing specificity.[7] Recently a family of G-tetrad forming oligonucleotides was introduced[8] as potential anti-HIV therapeutic drugs where modified guanosines may have an important role within a stability–activity relationship. 8-Aza-3-deazaguanine modified nucleosides **2** and **4**–**8**[9,10] hold all (hydrogen) atoms necessary for base pairing in Watson–Crick or Hoogsteen mode with reference to parent dG (**1**) and G (**3**), but their proton-donor and -acceptor capabilities, stacking properties and pK_a values are modified (Scheme 1). In addition, the isosteric and isoelectronic 3/8-C/N modification is expected[11–16] to influence the sugar puckering. The sugar moieties of nucleosides are involved in a dynamic two-state North (N) $\rightleftharpoons$ South (S) equilibrium.[17,18] The nucleobase at the anomeric centre drives the N $\rightleftharpoons$ S equilibria in **1**–**8** with two counteracting contributions: (i) steric effects, which are determined by the shape and size of the aglycon, and (ii) the anomeric effect,[19–21] which depends on the π-electron density of the individual heterocyclic moiety.[22–44] The O4′–C1′–N9 anomeric effect stabilizes the N-type sugar conformation in **1**–**8**, where the nucleobase occupies a pseudoaxial orientation, whereas the steric interactions of the heterocyclic nucleobase are minimized in the S-type pseudorotamer, where the

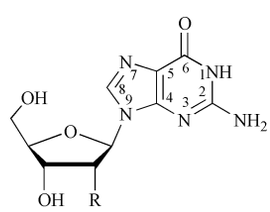

1: dG (R=H)
3: G (R=OH)

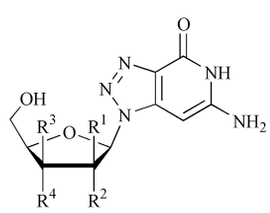

2: 8a3d-dG (R^1=R^2=R^3=H, R^4=OH)
4: 8a3d-G (R^1=R^3=H, R^2=R^4=OH)
5: 8a3d-araG (R^1=R^4=OH, R^2=R^3=H)
6: 8a3d-FaraG (R^1=F, R^2=R^3=H, R^4=OH)
7: 8a3d-xyloG (R^1=R^4=H, R^2=R^3=OH)
8: 8a3d-3dG (R^1=R^3=R^4=H, R^2=OH)

Scheme 1

DOI: 10.1039/b009401n

nucleobase occupies a pseudoequatorial orientation. A change in a sugar puckering is obviously induced by the introduction of a nitrogen atom into position 8 of a purine and leads to a distortion of the torsion angle about the N–glycosyl bond (χ).[4] A longer N9–C1′ bond in this general category of 8-azapurine nucleosides may induce striking peculiarities of their sugar moiety structure in the case where the N3-nitrogen atom is substituted by a lipophilic C–H or alkyl substituents.[3]

We expect that detailed temperature-dependent conformational analysis of 8-aza-3-deazaguanine nucleosides **2** and **4**–**8** in comparison to parent dG (**1**) and G (**3**) will give a deeper insight into the driving of the sugar N ⇌ S equilibrium of the modified nucleosides as well as the intrinsic electronic changes that will be observed through the modifications in anomeric and *gauche* effects. The isoelectronic substitution of positions 3 and 8 of guanine might have an important influence on the other two rotational degrees of freedom: equilibrium across the glycosyl bond and three-state equilibrium across the C4′–C5′ bond (orientation of the 5′-hydroxy group) which can also affect the possibility of H-bonding[45] between 5′-OH and the nucleobase. It is important to establish the interdependence of different conformational equilibria that influence the secondary structure and stability of the modified oligodeoxynucleotides at the monomer level.

Results and discussion

^{1}H NMR analysis of dynamic conformational equilibria of 1–8 in solution

The solution conformation of **1**–**8** has been inferred from $^3J_{HH}$ coupling constants and 1D difference NOE enhancements. The analysis of the solution conformation of sugar moieties in **1**–**8** is based on $^3J_{1'2'}$, $^3J_{1'2''}$, $^3J_{2'3'}$, $^3J_{2'3''}$, $^3J_{2''3''}$, $^3J_{3'4'}$ and $^3J_{3''4'}$ proton–proton coupling constants which have been acquired as a function of temperature from 298 to 358 K in 20 K steps (Table 1). $^3J_{HH}$ coupling constants were interpreted in terms of a two-state N ⇌ S pseudorotational equilibrium with the use of the computer program PSEUROT,[46,47] which calculates the least-squares fit of the five parameters defining the two-state N ⇌ S equilibrium (P_N, Ψ_m^N, P_S, Ψ_m^S and x_S) to the set of experimental $^3J_{HH}$. The conformational analyses of **1**–**8** have been performed primarily by constraining Ψ_m^N and Ψ_m^S to fixed values between 26 and 40° while optimising the phase angles of pseudorotation and respective populations of N- and S-type pseudorotamers (Table 2). After convergence we obtained the best fits between the experimental and back-calculated $^3J_{HH}$ coupling constants (root-mean-square error < 0.2 Hz, ΔJ_{max} < 0.2 Hz) for the N ⇌ S pseudorotational equilibria in **1**–**8**. The populations of the individual conformers at four temperatures in the range 298 to 358 K in 20 K steps have been used to calculate the enthalpy and entropy of the N ⇌ S pseudorotational equilibrium in **1**–**8** by making van't Hoff plots (Fig. 1).

S-type sugar conformations of guanine nucleosides dG (**1**) and G (**3**) are stabilized by $\Delta H°$ values of −2.4 and −2.6 kJ mol^{-1}, respectively, which are opposed by the weaker entropy contributions (Table 3). $\Delta H°$ and the counteracting entropy contributions are of comparable strength in 8a3d-dG (**2**), 8a3d-G (**4**) and 8a3d-xyloG (**7**) at 298 K, which results in a *ca.* 1 : 1 ratio of N and S conformers (Table 3). Positive $\Delta H°$ values in guanine modified nucleosides 8a3d-araG (**5**), 8a3d-FaraG (**6**) and 8a3d-3dG (**8**) are in control of the conformational bias of over 68% towards N-type sugar conformation (Table 3).

Pseudorotational equilibria of 2′-deoxyguanosine (1) and guanosine (3) in DMSO-d$_6$ and D$_2$O

The N ⇌ S pseudorotational equilibria in dG (**1**) and G (**3**) have been extensively studied as a function of temperature and pH in aqueous solution.[22,26] In the present study the conformational preferences of 8-aza-3-deaza modified nucleosides **2** and **4**–**8** were analysed in DMSO-d$_6$ due to their poor solubility in water. Comparison of the populations of major S-type conformers at 298 K for dG (**1**) shows only minor differences of 3% (73% in DMSO-d$_6$ and 70% in D$_2$O) due to change of solvent (Table 3). Similarly, G (**3**) exhibits only minor conformational changes of 3% upon the change of solvent from DMSO-d$_6$ (68% preference for S-type pseudorotamers) to D$_2$O (65%), respectively. The differences in respective $\Delta H°$ values were 0.4 and 0.7 kJ mol^{-1} for dG (**1**) and G (**3**), respectively and could be attributed to the following competing contributions: solvent dependent anomeric and *gauche* effects, differential solvation of hydroxy and other exocyclic groups, *etc*. The slight stabilization of N-type conformers in terms of the experimental $\Delta H°$ values (Table 3) in less polar DMSO-d$_6$ for both dG (**1**) and G (**3**) is consistent with the strengthening of the anomeric effect of the guanine nucleobase. The N ⇌ S equilibrium of dG (**1**) and G (**3**) in both solvents is, however, additionally tuned by the entropy contributions, which drive the N ⇌ S equilibrium towards N more efficiently in D$_2$O. The apparent strengthening of the anomeric effect of the guanine nucleobase in DMSO-d$_6$ in comparison to D$_2$O is smaller than 0.7 kJ mol^{-1}, which facilitates further explorations of the strengthening of the anomeric effect by 8-aza-3-deaza nucleobase modifications as in **2** and **4**–**8** in comparison to previous[22,33,39] quantitative evaluations of the anomeric effect of the parent guanine nucleobase in an aqueous medium.

8-Aza-3-deazaguanine modification strengthens the anomeric effect

Pairwise comparisons of the N ⇌ S equilibrium in 8a3d-dG (**2**) and 8a3d-G (**4**) with their natural counterparts dG (**1**) and G (**3**) showed that modified nucleosides exhibit a higher preference for N-type pseudorotamers by 20 and 13%, respectively (Table 3). The slopes and intercepts of the straight lines in Fig. 1 nicely illustrate the differences in thermodynamics of **1**–**2** (Fig. 1A) and **3**–**4** pairs (Fig. 1B). Stabilization of N-type pseudorotamers is evident from positive $\Delta\Delta H°$ values of 3.1 and 1.3 kJ mol^{-1} in 8a3d-dG (**2**) and 8a3d-G (**4**) in comparison to dG (**1**) and G (**3**), respectively. The stabilization of the N-type sugar conformation can be clearly attributed to the strengthening of the anomeric effect due to the more favourable overlap between the electron pair orbital of the endocyclic O4′ and the vacant antibonding σ* orbital of the glycosyl bond (*i.e.* $n_{O4'} \rightarrow \sigma^*_{C1'-N9}$ interactions). The redistribution of electron density from N9 into the pyridine moiety by the substitution of a carbon with a nitrogen on position 8 in 8a3d-dG (**2**) and 8a3d-G (**4**) makes N9 more electron deficient and results in the preferential stabilization of the pseudoaxially oriented nucleobase (N-type sugar conformation). The anomeric effect in 8a3d-dG (**2**) has been strengthened by 3.1 kJ mol^{-1} in comparison to the anomeric effect of guanine (16.4 kJ mol^{-1})[33] in dG (**1**). The anomeric effect of 8-aza-3-deazaguanine in 8a3d-dG (**2**) is therefore approximately 19.5 kJ mol^{-1} with the assumption that the steric effects of nucleobases in dG (**1**) and 8a3d-dG (**2**) are comparable.

In 8a3d-G (**4**), however, the anomeric effect is opposed by the *gauche* effect of the [N9–C1′–C2′–O2′] fragment, which drives the N ⇌ S equilibrium towards S. The apparent stabilization of the N-type pseudorotamers is reduced in 8a3d-G (**4**) to $\Delta\Delta H°$ of 1.3 kJ mol^{-1} as calculated from the comparison of $\Delta H°$ in G (**3**) and 8a3d-G (**4**). Comparison of $\Delta H°$ for 8a3d-G (**4**) with the parent G (**3**) shows that the anomeric effect and the *gauche* effect of the [N9–C1′–C2′–O2′] fragment have been simultaneously strengthened by 3.1 and 1.8 kJ mol^{-1}, respectively (Table 3).

Table 1 Vicinal proton–proton coupling constants and population of rotamers across the C4′–C5′ bond in **1**–**8** as a function of temperature in DMSO-d_6[a]

Compound	T/K	$J_{1'2'}$	$J_{1'2''}$	$J_{2'3'}$	$J_{2'3''}$	$J_{2''3'}$	$J_{3'4'}$	$J_{3''4'}$	$J_{4'5'}$	$J_{4'5''}$	%γ^+	%γ^t	%γ^-
dG (**1**)	298	7.9	6.0	5.7		3.0	2.7		4.7	4.7	40	30	30
	318	7.8	6.1	5.8		3.1	2.8		4.7	4.6	41	29	30
	338	7.7	6.1	5.9		3.2	2.9		4.6	4.6	42	29	29
	358	7.6	6.2	6.0		3.3	3.0		4.6	4.6	42	29	29
8a3d-dG (**2**)	298	5.8	6.7	6.4		4.6	3.9		5.5	5.9	19	42	39
	318	5.8	6.7	6.5		4.5	3.9		5.5	5.8	21	40	39
	338	5.9	6.7	6.6		4.5	3.9		5.4	5.8	21	41	38
	358	5.9	6.7	6.7		4.4	3.9		5.3	5.8	22	41	37
G (**3**)	298	6.1		5.1			3.5		4.1	4.1	52	24	24
	318	6.0		5.1			3.6		4.0	4.1	53	24	23
	338	5.9		5.2			3.6		4.0	4.2	52	25	23
	358	5.8		5.2			3.7		3.9	4.2	53	26	21
8a3d-G (**4**)	298	5.1		5.1			4.5		4.3	5.5	36	39	25
	318	5.0		5.2			4.5		4.4	5.5	35	39	26
	338	5.0		5.3			4.5		4.4	5.5	35	39	26
	358	4.9		5.4			4.5		4.4	5.5	35	39	26
8a3d-araG (**5**)	298	6.0		6.7			6.8		3.4	7.3	25	61	14
	318	5.9		6.4			6.8		3.5	6.9	29	56	15
	338	5.8		6.2			6.5		3.7	6.7	29	54	17
	358	5.7		6.1			6.4		3.8	6.5	30	51	19
8a3d-FaraG (**6**)[b]	298	5.4		5.1			6.5		4.1	6.7	25	53	22
	318	5.2		4.9			6.4		4.2	6.5	26	50	24
	338	5.2		4.8			6.4		4.3	6.4	26	49	25
	358	5.1		4.6			6.2		4.4	6.2	27	47	26
8a3d-xyloG (**7**)	298	4.1		3.9			5.1		4.2	6.9	22	55	23
	318	4.1		3.9			5.1		4.3	6.7	23	52	25
	338	4.1		3.9			5.1		4.4	6.5	24	50	26
	358	4.1		3.9			5.1		4.5	6.3	25	48	27
8a3d-3dG (**8**)	298	1.8		5.8	2.2		9.1	6.5	4.2	6.2	29	47	24
	318	1.9		5.9	2.3		9.1	6.5	4.3	6.1	29	46	25
	338	2.0		5.9	2.4		9.0	6.5	4.4	6.0	29	45	26
	358	2.1		6.0	2.5		9.0	6.5	4.5	5.9	29	43	28

[a] $^3J_{HH}$ (±0.1 Hz) are in Hz. Geminal proton–proton coupling constants were not sensitive to the change of temperature and were: $J_{2'2''} = -13.2$ in **1**, $J_{2'2''} = -13.4$ in **2**, $J_{3'3''} = -13.4$ in **8**, $J_{5'5''} = -11.8$ in **1**, −11.5 in **2**, −12.0 in **3**, −11.8 in **4**, −11.7 in **5**, −11.9 in **6**, −11.8 in **7** and −11.7 Hz in **8**. [b] Proton–fluorine coupling constants in **6** were: $J_{1',2'F} = 10.4$ (298 K), 10.9 (318 K), 11.3 (338 K) and 11.6 Hz (358 K). Proton–fluorine coupling constants which were not sensitive to the change of temperature were: $J_{2',2'F} = -52.9$, $J_{3',2'F} = 19.6$ and $J_{2'F,4'} = 0.9$ Hz.

Are 8-aza-3-deaza modifications altering the *gauche* effects of hydroxy groups?

The *gauche* effect of the 3′-OH group in 8a3d-G (**4**) estimated by the subtraction of $\Delta H°$ values for 8a3d-3dG (**8**) from 8a3d-G (**4**) is −5.2 kJ mol^{-1}. This estimate of the *gauche* effect of the [O4′–C4′–C3′–O3′] fragment in the 8-aza-3-deaza modified nucleoside is comparable to the estimate of −5.7 kJ mol^{-1} from the comparison of 3′-dA and A.[39] The driving of the N ⇌ S equilibrium towards S by the *gauche* effect of the [O4′–C4′–C3′–O3′] fragment in the absence of the 2′-OH group has shown the following variation with the nucleobase: −7.4 and −6.2 kJ mol^{-1} for ddA–dA and ddG–dG pairs, respectively.[39] We can therefore conclude that the *gauche* effect of the 3′-OH group in **2** and **4**–**6** is not affected by the 8-aza-3-deaza modification of the nucleobase.

The driving of the N ⇌ S equilibrium by the 3′-OH group on the sterically more crowded β-side of the sugar moiety in 8a3d-xyloG (**7**) towards S-type conformers by −3.9 kJ mol^{-1} has been determined by subtraction of $\Delta H°$ values for 8a3d-xyloG (**7**) from 8a3d-3dG (**8**). The driving of the N ⇌ S equilibrium in 8a3d-xyloG (**7**) by 3′-OH is the result of several competing interactions due to its involvement in the *gauche* effects of [O4′–C4′–C3′–O3′] (prefers N) and [O3′–C3′–C2′–O2′] (prefers S) fragments and steric effects with the nucleobase, which are minimized in the S-type conformation (pseudoequatorial orientation of 3′-OH).

The conformational analysis of arabino nucleosides 8a3d-araG (**5**) and 8a3d-FaraG (**6**) showed a high conformational bias of 85% and 68% towards N-type, respectively at 298 K. The van't Hoff analysis showed that the N ⇌ S equilibrium in both 8a3d-araG (**5**) and 8a3d-FaraG (**6**) is driven towards N by large $\Delta H°$ values (Table 3). The anomeric effect of the nucleobase and the *gauche* effect of the [O3′–C3′–C2′–O2′/F2′] fragment stabilize N-type conformers and are opposed by the weaker steric effects of the nucleobase and the *gauche* effects of the [O4′–C1′–C2′–O2′/F2′] and [O4′–C4′–C3′–O3′] fragments. A simple molecular modeling has shown that [N9–C1′–C2′–O2′/F2′] fragments adopt *gauche-minus* and *gauche-plus* conformations in N- and S-type conformations of 8a3d-araG (**5**) and 8a3d-FaraG (**6**), respectively. It could therefore be expected that the *gauche* effects of [N9–C1′–C2′–O2′/F2′] fragments do not preferentially stabilize either of the pseudorotamers in 8a3d-araG (**5**) and 8a3d-FaraG (**6**). The effect of 2′-substituents in 8a3d-araG (**5**) and 8a3d-FaraG (**6**) on the N ⇌ S equilibrium can be estimated by the comparison of $\Delta H°$ values in the following pairs of nucleosides: (i) the comparison of 8a3d-dG (**2**) and 8a3d-araG (**5**) gives the estimate of +7.0 kJ mol^{-1} for the effect of 2′-OH on the N ⇌ S equilibrium in 8a3d-araG (**5**) and (ii) the comparison of 8a3d-dG (**2**) and 8a3d-FaraG (**6**) yields +2.3 kJ mol^{-1} for the effect of 2′-F on the N ⇌ S equilibrium in 8a3d-FaraG (**6**). The smaller $\Delta\Delta H°$ drive towards N in 8a3d-FaraG (**6**) cannot be explained by the consideration of the *gauche* effect of [O–C–C–F] being stronger than that of the [O–C–C–O] fragment.[24] It is noteworthy that similar comparison of the effects of 2′-OH and 2′-F on the N ⇌ S equilibrium in arabino-adenosine analogues showed 40%[48] more stabilization of N-type pseudorotamers at 298 K in the former. The dramatic difference in comparison to the 8a3d-

araG (**5**)–8a3d-FaraG (**6**) pair ($\Delta = 17\%$, Table 3) suggests some sort of interaction (possibly electrostatic) of 8-aza-3-deazaguanine with the 2′-fluorine atom which less strongly stabilizes S-type conformers in the 8-aza-3-deaza analogue. The anomeric effect of 8-aza-3-deazaguanine (≈19.5 kJ mol^{-1}) is considerably stronger than the anomeric effect of adenine (14.7 kJ mol^{-1}),[33] which has an important impact on the hybridisation state of C1′. The ratio of the sp^3 *vs.* sp^2 nature of C1′ influences the *gauche* effects where C1′ is the intervening atom as in [N9–C1′–C2′–O2′/F2′] fragments in 8a3d-araG (**5**) and 8a3d-FaraG (**6**). On the other hand, electronegative fluorine exerts an electron-withdrawing effect and back donation on the neighbouring atoms, thus changing their p character and deforming their bond lengths and bond angles.[49–52] An important factor in the evaluation of the *gauche* effects of [O3′–C3′–C2′–F2′] and [O4′–C1′–C2′–F2′] fragments is that only the former can be strengthened by OH···F hydrogen bonding[53] in 8a3d-FaraG (**6**) which can considerably contribute to the driving of the N⇌S equilibrium.

Comparison of $\Delta H°$ values for 8a3d-dG (**2**) and 8a3d-G (**4**) shows that the 2′-OH group on the α-side of the pentofuranosyl moiety drives the N⇌S equilibrium in 8a3d-G (**4**) towards S by −2.0 kJ mol^{-1}. Comparison of dG (**1**) and G (**3**) shows that the 2′-OH group stabilizes S-type conformers by $\Delta\Delta H°$ of −0.2 kJ mol^{-1} in the latter. The difference of 1.8 kJ mol^{-1} can be safely attributed to the fact that the *gauche* effect of the [N9–C1′–C2′–O2′] fragment is stronger when N9 is part of the triazolo moiety in 8a3d-G (**4**) in comparison to the imidazolo moiety in G (**3**).

Conformational equilibrium across the C1′–N9 (χ) bond in 1–8

1D difference NOE experiments were performed to assess the preferred conformation around the glycosyl (C1′–N9) bond in **1**–**8** (Table 4). The guanine base in dG (**1**) and G (**3**) in DMSO-d_6 prefers the *anti* position.[54] The NOE enhancements upon saturation of H3 in 8-aza-3-deazaguanine modified nucleosides[10] **2** and **4**–**8** were larger at H1′ than at H2′, except in 8a3d-xyloG (**7**). NOE enhancements in Table 4 show that 8-aza-3-deazaguanine thus prefers a predominantly *anti* or *high-anti* orientation with regard to the sugar ring in **2** and **4**–**8** which is similar to its natural counterpart guanine in dG (**1**) and G (**3**) in DMSO-d_6.

Conformational equilibrium across the C4′–C5′ (γ) bond in 1–8

Conformational analysis of $^3J_{4'5'}$ and $^3J_{4'5''}$ coupling constants has shown that γ^t rotamers are the most highly populated of the three rotamers in the $\gamma^+ \rightleftharpoons \gamma^t \rightleftharpoons \gamma^-$ equilibrium[55] in 8-aza-3-deazaguanine nucleosides **2** and **4**–**8** at 298 K (Table 1). Inspection and comparison of the populations of γ rotamers in dG (**1**) and G (**3**) with those in 8a3d-dG (**2**) and 8a3d-G (**4**), respectively show that 8-aza-3-deaza modification leads to an increase in the population of γ^t and a decrease in the population of γ^+ rotamers. γ^t rotamers are also preferred in **5**–**8** (Table 1). It is noteworthy that the larger population of γ^t rotamers in **1**–**8** correlates with the larger population of N-type conformers, whereas the larger population of γ^+ rotamers correlates with the larger population of S-type conformers (Tables 1 and 2). The above interdependence of N-γ^t and S-γ^+ conformational equilibria in **1**–**8** is consistent with the previous correlations in 8-aza-7-deaza-2′-deoxyguanosine.[12] In 2′-fluorinated nucleoside derivatives, however, the larger drive towards N and the higher preference for γ^t rotamers in 8a3d-araG (**5**) compared to 8a3d-FaraG (**6**) is in contradistinction to the correlations of N sugar puckering and the higher preference for γ^+ rotamers in adenine nucleosides.[48] We have observed no sign of interaction between 5′-OH and H-bonding acceptors on the heterocycle in **1**–**8**, which would potentially influence γ rotamer populations.

Table 2 Conformational analysis of N⇌S pseudorotational equilibrium in **1**–**8** in DMSO-d_6

Compound	Geometries of N- and S-type conformers				Error of pseud. analysis		Population of N-type conformers[a]		
	P_N/°	Ψ_m^N/°	P_S/°	Ψ_m^S/°	r.m.s./Hz	ΔJ_{max}/Hz	%N (298 K)	%N (318 K)	%N (338 K)	%N (358 K)
dG (**1**)	4–10	33–35	157	33–35	<0.1	<0.1	26–27	27–28	28–29	29–30
8a3d-dG (**2**)	−4–−2	30–31	153–155	30–31	<0.1	0.2	47–48	47–48	46–47	46–47
G (**3**)	30–36	31–32	152–156	31–32	<0.1	0.2	31–33	32–34	33–35	35–37
8a3d-G (**4**)	22–34	31	145–155	31	<0.1	0.2	43–46	44–47	44–47	46–49
8a3d-araG (**5**)	−12–4	40	137–180	40	0.1	0.2	80–88	78–86	74–82	72–80
8a3d-FaraG (**6**)	1–26	38–40	130–175	38–40	<0.1	<0.1	68–69	65–66	64–65	63–64
8a3d-xyloG (**7**)	−27–20	26–36	181–141	26–36	<0.1	<0.1	46–58	46–58	46–58	46–58
8a3d-3dG (**8**)	−2–8	29–32	119–130	29–32	<0.2	0.3	74–77	72–75	70–74	69–72

[a] Individual population sets were used in the calculation of individual van't Hoff plots (Fig. 1).

Table 3 Thermodynamic parameters for N ⇌ S pseudorotational equilibrium in **1**–**8** in DMSO-d_6

Compound	$\Delta H°$/kJ mol^{-1}	$\Delta S°$/J K^{-1} mol^{-1}	$-T\Delta S°$ (298 K)/kJ mol^{-1}	$\Delta G^{298\ K}$/kJ mol^{-1}	%N (298 K)
dG (**1**)	−2.4 (σ = 0.1)	0.2 (σ = 0.1)	−0.1	−2.5	27
dG (**1**)[a]	−2.8 (σ = 0.2)	−3.6 (σ = 0.7)	1.1	−1.7	30
8a3d-dG (**2**)	0.7 (σ = 0.1)	3.0 (σ = 0.1)	−1.0	−0.3	47
G (**3**)	−2.6 (σ = 0.1)	−2.4 (σ = 0.2)	0.7	−1.9	32
G (**3**)[a]	−3.3 (σ = 0.2)	−6.2 (σ = 0.7)	1.8	−1.5	35
8a3d-G (**4**)	−1.3 (σ = 0.1)	−2.5 (σ = 0.4)	0.8	−0.5	45
8a3d-araG (**5**)	7.7 (σ = 1.6)	11.3 (σ = 3.0)	−3.4	4.3	85
8a3d-FaraG (**6**)	3.0 (σ = 0.1)	3.8 (σ = 0.4)	−1.1	1.9	68
8a3d-xyloG (**7**)	0.0 (σ = 0.1)	−0.9 (σ = 1.2)	0.3	0.3	53
8a3d-3dG (**8**)	3.9 (σ = 0.1)	3.8 (σ = 0.7)	−1.1	2.8	76

[a] Pseudorotational analysis has been performed in D_2O.[26]

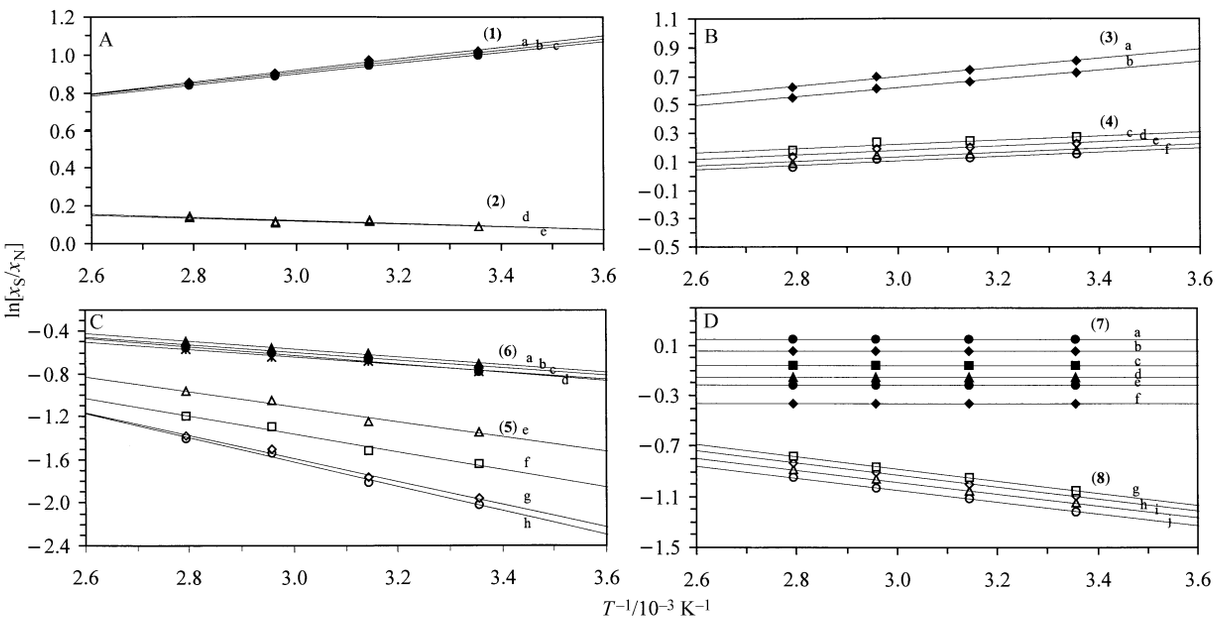

Fig. 1 van't Hoff plots of ln(x_S/x_N) as a function of 1000/T for dG (**1**; line **a** corresponds to $P_N = 4° \rightleftharpoons P_S = 157°$, $\Psi_m{}^N = \Psi_m{}^S = 33°$; **b** corresponds to $P_N = 6° \rightleftharpoons P_S = 157°$, $\Psi_m{}^N = \Psi_m{}^S = 34°$; **c** corresponds to $P_N = 10° \rightleftharpoons P_S = 157°$, $\Psi_m{}^N = \Psi_m{}^S = 35°$) and 8a3d-dG (**2**; **d** corresponds to $P_N = -4° \rightleftharpoons P_S = 153°$, $\Psi_m{}^N = \Psi_m{}^S = 31°$; **e** corresponds to $P_N = -1.9° \rightleftharpoons P_S = 155°$, $\Psi_m{}^N = \Psi_m{}^S = 30°$) in panel [A], for G (**3**; line **a** corresponds to $P_N = 30° \rightleftharpoons P_S = 152°$, $\Psi_m{}^N = \Psi_m{}^S = 31°$; **b** corresponds to $P_N = 36° \rightleftharpoons P_S = 156°$, $\Psi_m{}^N = \Psi_m{}^S = 32°$) and 8a3d-G (**4**; **c** corresponds to $P_N = 22° \rightleftharpoons P_S = 145°$, $\Psi_m{}^N = \Psi_m{}^S = 31°$; **d** corresponds to $P_N = 26° \rightleftharpoons P_S = 148°$, $\Psi_m{}^N = \Psi_m{}^S = 31°$; **e** corresponds to $P_N = 31° \rightleftharpoons P_S = 152°$, $\Psi_m{}^N = \Psi_m{}^S = 31°$; **f** corresponds to $P_N = 34° \rightleftharpoons P_S = 155°$, $\Psi_m{}^N = \Psi_m{}^S = 31°$) in panel [B], for 8a3d-FaraG (**6**; line **a** corresponds to $P_N = 15° \rightleftharpoons P_S = 139°$, $\Psi_m{}^N = \Psi_m{}^S = 39°$; **b** corresponds to $P_N = 26° \rightleftharpoons P_S = 149°$, $\Psi_m{}^N = \Psi_m{}^S = 40°$; **c** corresponds to $P_N = 39° \rightleftharpoons P_S = 175°$, $\Psi_m{}^N = \Psi_m{}^S = 42°$; **d** corresponds to $P_N = 1° \rightleftharpoons P_S = 130°$, $\Psi_m{}^N = \Psi_m{}^S = 38°$) and 8a3d-araG (**5**; line **e** corresponds to $P_N = -3° \rightleftharpoons P_S = 160°$, $\Psi_m{}^N = \Psi_m{}^S = 40°$; **f** corresponds to $P_N = 4°$, $\Psi_m{}^N = 41° \rightleftharpoons P_S = 180°$, $\Psi_S = 40°$; **g** corresponds to $P_N = -11° \rightleftharpoons P_S = 140°$, $\Psi_m{}^N = \Psi_m{}^S = 40°$; **h** corresponds to $P_N = -12° \rightleftharpoons P_S = 137°$, $\Psi_m{}^N = \Psi_m{}^S = 40°$) in panel [C], for 8a3d-xyloG (**7**; line **a** corresponds to $P_N = 20° \rightleftharpoons P_S = 181°$, $\Psi_m{}^N = \Psi_m{}^S = 26°$; **b** corresponds to $P_N = 10° \rightleftharpoons P_S = 172°$, $\Psi_m{}^N = \Psi_m{}^S = 27°$; **c** corresponds to $P_N = -6° \rightleftharpoons P_S = 159°$, $\Psi_m{}^N = \Psi_m{}^S = 29°$; **d** corresponds to $P_N = -15° \rightleftharpoons P_S = 152°$, $\Psi_m{}^N = \Psi_m{}^S = 31°$; **e** corresponds to $P_N = -21° \rightleftharpoons P_S = 147°$, $\Psi_m{}^N = \Psi_m{}^S = 33°$; **f** corresponds to $P_N = -27° \rightleftharpoons P_S = 141°$, $\Psi_m{}^N = \Psi_m{}^S = 36°$) and 8a3d-3dG (**8**; line **g** corresponds to $P_N = -2° \rightleftharpoons P_S = 119°$, $\Psi_m{}^N = \Psi_m{}^S = 32°$; **h** corresponds to $P_N = 2° \rightleftharpoons P_S = 122°$, $\Psi_m{}^N = \Psi_m{}^S = 31°$; **i** corresponds to $P_N = 5° \rightleftharpoons P_S = 126°$, $\Psi_m{}^N = \Psi_m{}^S = 30°$; **j** corresponds to $P_N = 8° \rightleftharpoons P_S = 130°$, $\Psi_m{}^N = \Psi_m{}^S = 29°$) in panel [D].

Experimental

NMR spectroscopy

^{1}H NMR spectra were recorded at 299.942 MHz on a Varian Unity Plus NMR spectrometer at the National NMR Center of Slovenia. Samples were dissolved in DMSO-d_6 (99.9% deuterium) due to poor solubility in D_2O. Sample concentrations were approx. 50 mM for all samples. Resonances of G (**3**), 8a3d-araG (**5**), 8a3d-xyloG (**7**) and 8a3d-3dG (**8**) were broad. After addition of approx. 100 μl of D_2O and exchange of hydroxy protons, the spectra simplified and individual $^3J_{HH}$ coupling constants could be extracted. ^{1}H NMR spectra of 8a3d-araG (**5**) and 8a3d-xyloG (**7**) were recorded before and after addition of D_2O. The change in $^3J_{HH}$ coupling constants was smaller than 0.05 Hz, which indicates that the influence of a small addition of D_2O to DMSO-d_6 solution on the conformational equilibria is negligible. Spectra were acquired at four temperatures from 298 to 358 K (±0.5 K) in 20 K steps. In order to obtain accurate J-coupling data and chemical shifts all ^{1}H NMR spectra were simulated with a standard computer simulation algorithm (VNMR rev. 6.1A).[56] The error in $^3J_{HH}$ is smaller than 0.1 Hz as estimated from comparison of the experimental and simulated spectra.

Conformational analysis of $^3J_{HH}$ coupling constants

The conformational analysis of the pentofuranose moiety in **1**–**8** has been performed with the use of the computer program PSEUROT[46] which finds the best fit between experimental and calculated $^3J_{HH}$. The input consists of the parameters P_1–P_6 for the generalized Karplus–Altona equation,[57] the λ electronegativities of the four substituents, A, B parameters, temperature-dependent experimental $^3J_{HH}$ and the initial guesses of the geometries of the starting conformers and their

Table 4 1D ^{1}H NOE enhancements

Compound	H saturated	NOE enhancements (%)
dG (**1**)[a]	H8	H1′(3.1); H2′(3.7); H3′(1.1)
8a3d-dG (**2**)	H3	H1′(7.8); H2′(1.4); H3′(0.9)
G (**3**)[a]	H8	H1′(3.6); H2′(5.7); H3′(1.1)
8a3d-G (**4**)	H3	H1′(8.1); H2′(3.5); H3′(0.3)
8a3d-araG (**5**)	H3	H1′(4.0); H3′(2.1)
8a3d-FaraG (**6**)	H3	H1′(5.5); H2′(0.6); H3′(2.0)
8a3d-xyloG (**7**)	H3	H1′(4.3); H2′(4.4); 3′-OH(0.3)
8a3d-3dG (**8**)	H3	H1′(12.0); H2′(1.2); H3′(0.6)

[a] Data from ref. 54.

respective populations. The following λ electronegativity values were used: 0.0 for H, 1.39 for OH, 0.62 for C1′, C3′ and C4′, 0.67 for C2′ in **1** and **2** and for C3′ in **8**, 0.68 for C5′, 1.37 for F and 0.58 for the nucleobase. The λ electronegativity for the modified nucleobase was varied by ±0.1 in the three sets of conformational analyses by the PSEUROT program in order to assess its effect on the analysis of $^3J_{HH}$ coupling constants. The results, however, showed only a slight variation of the geometries of the puckered pseudorotamers ($-8° < P_N < 4°$, $151° < P_S < 157°$, $30° < \Psi_m^N = \Psi_m^S < 31°$ for 8a3d-dG (**2**)), while population ($\Delta < 2\%$) and thermodynamic parameters ($\Delta\Delta H° < 0.1$ kJ mol^{-1}, $\Delta\Delta S° < 0.3$ J mol^{-1} K^{-1}) varied within the experimental error.

Acknowledgements

We thank the Ministry of Education, Science and Sports of the Republic of Slovenia (Program No. P1–0515 and Grant No. Z1–8609–0104) and European Commission (Contract No. ICA1-CT–2000–70034) for their financial support.

References

1 G. R. Revankar, P. K. Gupta, A. D. Adams, N. K. Dalley, P. A. McKernan, P. D. Cook, P. G. Canonico and R. K. Robins, *J. Med. Chem.*, 1984, **27**, 1389.
2 M. S. Poonian, W. W. McComas and M. J. Kramer, *J. Med. Chem.*, 1979, **22**, 958.
3 O. L. Acevedo, R. S. Andrews and P. D. Cook, *Nucleosides Nucleotides*, 1993, **12**, 403.
4 P. Singh and D. J. Hodgson, *J. Am. Chem. Soc.*, 1974, **96**, 5276.
5 F. Seela, H. Debelak, N. Usman, A. Burgin and L. Beigelman, *Nucleic Acids Res.*, 1998, **26**, 1010.
6 M. R. Player, E. N. Kalinichenko, T. L. Podkopaeva, I. A. Mikhailopulo, F. Seela and P. F. Torrence, *Biochem. Biophys. Res. Commun.*, 1998, **245**, 430.
7 S. T. Crooke, *Methods Enzymol.*, 2000, **313**, 3.
8 N. Jing, E. De Clercq, R. F. Rando, L. Pallansch, C. Lackman-Smith, S. Lee and M. E. Hogan, *J. Biol. Chem.*, 2000, **275**, 3421.
9 A. Stimac, I. Leban and J. Kobe, *Synlett*, 1999, **7**, 1069.
10 Purine numbering has been used throughout the manuscript for 1,2,3-triazolo[4,5-*c*]pyridine nucleobase.
11 F. Seela, H. Rosemeyer, M. Zulauf, Y. M. Chen, G. Kastner and H. Reuter, *Liebigs Ann./Recl.*, 1997, 2525.
12 H. Rosemeyer and F. Seela, *J. Chem. Soc., Perkin Trans. 2*, 1997, 2341.
13 H. Rosemeyer, M. Zulauf, N. Ramzaeva, G. Becher, E. Feiling, K. Muhlegger, I. Munster, A. Lohmann and F. Seela, *Nucleosides Nucleotides*, 1997, **16**, 821.
14 F. Seela, H. Debelak, H. Reuter, G. Kastner and I. A. Mikhailopulo, *Tetrahedron*, 1999, **55**, 1295.
15 F. Seela and A. Melenewski, *Eur. J. Org. Chem.*, 1999, 485.
16 F. Seela, G. Becher, H. Rosemeyer, H. Reuter, G. Kastner and I. A. Mikhailopulo, *Helv. Chim. Acta*, 1999, **82**, 105.
17 C. Altona and M. Sundaralingam, *J. Am. Chem. Soc.*, 1973, **95**, 2333.
18 C. Altona and M. Sundaralingam, *J. Am. Chem. Soc.*, 1972, **94**, 8205.
19 I. Tvaroska and T. Bleha, *Anomeric and exo-anomeric effects in carbohydrate chemistry*, Vol. 47, Academic Press, San Diego, 1989.
20 E. Juaristi and G. Cuevas, *Tetrahedron*, 1992, **48**, 5019.
21 A. J. Kirby and N. H. Williams, in *The Anomeric Effect and Associated Stereoelectronic Effects*, G. R. J. Thatcher, Ed.; American Chemical Society, ACS Symposium Series, 539 edn., Washington, DC, 1993, p. 55.
22 J. Plavec, W. Tong and J. Chattopadhyaya, *J. Am. Chem. Soc.*, 1993, **115**, 9734.
23 C. Thibaudeau, J. Plavec, K. A. Watanabe and J. Chattopadhyaya, *J. Chem. Soc., Chem. Commun.*, 1994, 537.
24 C. Thibaudeau, J. Plavec, N. Garg, A. Papchikhin and J. Chattopadhyaya, *J. Am. Chem. Soc.*, 1994, **116**, 4038.
25 C. Thibaudeau, J. Plavec and J. Chattopadhyaya, *J. Am. Chem. Soc.*, 1994, **116**, 8033.
26 C. Thibaudeau, J. Plavec and J. Chattopadhyaya, *J. Org. Chem.*, 1996, **61**, 266.
27 J. Plavec, C. Thibaudeau and J. Chattopadhyaya, *Pure Appl. Chem.*, 1996, **68**, 2137.
28 C. Thibaudeau, A. Földesi and J. Chattopadhyaya, *Tetrahedron*, 1997, **53**, 14043.
29 C. Thibaudeau and J. Chattopadhyaya, *Nucleosides Nucleotides*, 1997, **16**, 523.
30 I. Luyten, C. Thibaudeau, A. Sandström and J. Chattopadhyaya, *Tetrahedron*, 1997, **53**, 6433.
31 I. Luyten, C. Thibaudeau and J. Chattopadhyaya, *J. Org. Chem.*, 1997, **62**, 8800.
32 J. Plavec, P. Roselt, A. Földesi and J. Chattopadhyaya, *Magn. Reson. Chem.*, 1998, **36**, 732.
33 M. Polak, B. Mohar, J. Kobe and J. Plavec, *J. Am. Chem. Soc.*, 1998, **120**, 2508.
34 C. Thibaudeau, A. Földesi and J. Chattopadhyaya, *Tetrahedron*, 1998, **54**, 1867.
35 C. Thibaudeau, A. Kumar, S. Bekiroglu, A. Matsuda, V. E. Marquez and J. Chattopadhyaya, *J. Org. Chem.*, 1998, **63**, 5447.
36 C. Thibaudeau and J. Chattopadhyaya, *Nucleosides Nucleotides*, 1998, **17**, 1589.
37 M. Polak and J. Plavec, *Nucleosides Nucleotides*, 1998, **17**, 2011.
38 M. Polak, J. Plavec, A. Trifonova, A. Földesi and J. Chattopadhyaya, *J. Chem. Soc., Perkin Trans. 1*, 1999, 2835.
39 C. Thibaudeau and J. Chattopadhyaya, *Stereoelectronic Effects in Nucleosides and Nucleotides and their Structural Implications*, Uppsala University Press, Uppsala, Sweden, 1999.
40 P. Acharya, A. Trifonova, C. Thibaudeau, A. Földesi and J. Chattopadhyaya, *Angew. Chem., Int. Ed.*, 1999, **38**, 3645.
41 M. Polak and J. Plavec, *Nucleosides Nucleotides*, 1999, **18**, 1109.
42 M. Polak and J. Plavec, *Eur. J. Inorg. Chem.*, 1999, 547.
43 P. Acharya, B. Nawrot, M. Sprinzl, C. Thibaudeau and J. Chattopadhyaya, *J. Chem. Soc., Perkin Trans. 2*, 1999, 1531.
44 M. Crnugelj, D. Dukhan, J. L. Barascut, J. L. Imbach and J. Plavec, *J. Chem. Soc., Perkin Trans. 2*, 2000, 255.
45 F. Seela, H. Debelak, H. Reuter, G. Kastner and I. A. Mikhailopulo, *Nucleosides Nucleotides*, 1998, **17**, 729.
46 C. Haasnoot, F. A. A. M. de Leeuw, D. Huckriede, J. van Wijk and C. Altona, PSEUROT – A program for the conformational analysis of five membered rings, version 6.0, Leiden, Netherlands, 1993.
47 F. A. A. M. de Leeuw and C. Altona, *J. Comput. Chem.*, 1983, **4**, 428.
48 H. Ford, F. Dai, L. Mu, M. A. Siddiqui, M. C. Nicklaus, L. Anderson, V. E. Marquez and J. J. Barchi, *Biochemistry*, 2000, **39**, 2581.
49 K. B. Wiberg, *Acc. Chem. Res.*, 1994, **29**, 229.
50 N. C. Craig, A. Chen, K. H. Suh, S. Klee, G. C. Mellau, B. P. Winnewisser and M. Winnewisser, *J. Am. Chem. Soc.*, 1997, **119**, 4789.
51 Y. P. Chang, T. M. Su, T. W. Li and I. Chao, *J. Phys. Chem. A*, 1997, **101**, 6107.
52 O. Engkvist, G. Karlstrom and P. O. Widmark, *Chem. Phys. Lett.*, 1997, **265**, 19.
53 R. J. Abraham, T. A. D. Smith and W. A. Thomas, *J. Chem. Soc., Perkin Trans. 2*, 1996, 1949.
54 H. Rosemeyer, G. Toth, B. Golankiewicz, Z. Kazimierczuk, W. Bourgeois, U. Kretschmer, H.-P. Muth and F. Seela, *J. Org. Chem.*, 1990, **55**, 5784.
55 C. A. G. Haasnoot, F. A. A. M. de Leeuw, H. P. M. de Leeuw and C. Altona, *Recl. Trav. Chim. Pays-Bas*, 1979, **98**, 576.
56 Varian, VNMR™ data acquisition and processing software, revision 6.1A, Palo Alto, USA, 1999.
57 C. Altona, R. Francke, R. de Haan, J. H. Ippel, G. J. Daalmans, A. J. A. Westra Hoekzema and J. van Wijk, *Magn. Reson. Chem.*, 1994, **32**, 670.